Active One-Way Quantum Computation with Two-Photon Four-Qubit Cluster States

Giuseppe Vallone,* Enrico Pomarico,† Francesco De Martini,* and Paolo Mataloni*

Dipartimento di Fisica, "Sapienza" Università di Roma and Consorzio Nazionale Interuniversitario per le Scienze Fisiche della Materia, Roma, 00185 Italy

(Received 11 December 2007; published 22 April 2008)

By using 2-photon 4-qubit cluster states we demonstrate deterministic one-way quantum computation in a single qubit rotation algorithm. In this operation feed-forward measurements are automatically implemented by properly choosing the measurement basis of the qubits, while Pauli error corrections are realized by using two fast driven Pockels cells. We realized also a C-NOT gate for equatorial qubits and a C-PHASE gate for a generic target qubit. Our results demonstrate that 2-photon cluster states can be used for rapid and efficient deterministic one-way quantum computing.

DOI: 10.1103/PhysRevLett.100.160502 PACS numbers: 03.67.Pp, 03.67.Lx, 03.67.Mn, 42.50.Dv

Cluster states are the basic resource for one-way quantum computation (QC) [1]. In the standard QC approach any quantum algorithm can be realized by a sequence of single qubit rotations and two-qubit gates, such as C-NOT and C-PHASE [2]. Deterministic one-way QC is based on the initial preparation of entangled qubits in a cluster state, followed by a temporally ordered pattern of single qubit measurements and feed-forward (FF) operations depending on the outcome of the already measured qubits [1]. We can consider two different types of FF operations: (i) the intermediate feed-forward measurements, i.e., the choice of the measurement basis depending on the previous measurement outcomes and (ii) the Pauli matrix feed-forward corrections on the final output state. Two-qubit gates can be realized by exploiting the existing entanglement between qubits. In this way the difficulties of standard QC, related to the implementation of two-qubit gates, are transferred to the preparation of the state.

One-way QC was experimentally realized by using 4-photon cluster states [3] and, later, by implementing Pauli error corrections with active feed forward [4]. Very recently, a proof of principle of one-way QC (namely, the Grover's search algorithm and a particular C-PHASE gate) was given by employing 2-photons entangled in a 4-qubit cluster state, without active feed forward [5]. The possibility of encoding more qubits on the same photon determines important advantages. For instance, the overall detection efficiency, and then the detection rate, is constant. In fact, in general it scales as η^N, with N the number of photons and η the detection efficiency for each photon. Moreover 2-photon cluster states, realized by entangling the polarization (π) and linear momentum ($\mathbf{k}$) degrees of freedom (DOF), outperform the earlier results obtained by 4-photon cluster states since the state fidelities can be far larger and the count rate can be higher by 3–4 orders of magnitude [5,6].

One may ask how feed-forward operations can be implemented in the case of 2-photon multiqubit cluster states and if the different DOF of the photons are computationally equivalent. In this Letter we demonstrate that a simple smart choice of the measurement basis can be used in this case to deterministically perform the single qubit rotation algorithm, instead of adopting intermediate active feed-forward measurements [type (i)], which are necessary in the case of QC with 4-photon cluster states [4]. Moreover feed-forward corrections [type (ii)] have been implemented in the same algorithm by using active fast driven electro-optics modulators. In this way, high speed deterministic one-way single qubit rotations are realized with 2-photon 4-qubit cluster states [7]. In the same context, we have also verified the equivalence existing between the polarization and linear momentum DOFs by using either $\mathbf{k}$ or π as QC output qubit.

Besides single qubit rotations, two-qubit gates, such as the C-NOT gate, are required for the realization of arbitrary quantum algorithms [2]. The realization of a C-NOT gate for equatorial qubits and a universal C-PHASE gate acting on arbitrary target qubits is also presented in this Letter.

In our experiment 2-photon 4-qubit cluster states were generated by using the methods described in [6,8–10], to which we refer for details. Two photons belonging to the cluster state [11]

$$|C_4\rangle = \tfrac{1}{2}(|H\ell\rangle_A|Hr\rangle_B - |Hr\rangle_A|H\ell\rangle_B + |Vr\rangle_A|V\ell\rangle_B + |V\ell\rangle_A|Vr\rangle_B) \quad (1)$$

are generated either with horizontal (H) or vertical (V) polarization, in the left (ℓ) or right (r) mode of the Alice (A) or Bob (B) side (see Fig. 1 of [6]). Cluster states were detected with fidelity $F = 0.880 \pm 0.013$, as obtained from the measurement of the stabilizer operators of $|C_4\rangle$ [12].

By the correspondence $|H\rangle \leftrightarrow |0\rangle$, $|V\rangle \leftrightarrow |1\rangle$, $|\ell\rangle \leftrightarrow |0\rangle$, $|r\rangle \leftrightarrow |1\rangle$, the state $|C_4\rangle$ is equivalent to the cluster state $|\Phi_4^{\mathrm{lin}}\rangle = \frac{1}{2}(|+\rangle_1|0\rangle_2|0\rangle_3|+\rangle_4 + |+\rangle_1|0\rangle_2|1\rangle_3|-\rangle_4 + |-\rangle_1|1\rangle_2|0\rangle_3|+\rangle_4 - |-\rangle_1|1\rangle_2|1\rangle_3|-\rangle_4)$ [13] [with $|\pm\rangle = \frac{1}{\sqrt{2}}(|0\rangle \pm |1\rangle)$] up to single qubit unitaries:

$$|C_4\rangle = U_1 \otimes U_2 \otimes U_3 \otimes U_4|\Phi_4^{\mathrm{lin}}\rangle \equiv \mathcal{U}|\Phi_4^{\mathrm{lin}}\rangle. \quad (2)$$

Here $|\Phi_4^{\text{lin}}\rangle$ and $|C_4\rangle$ are, respectively, expressed in the so-called "computational" and "laboratory" basis, while the U_j's ($j = 1, \ldots, 4$) are products of Hadamard gates $H = \frac{1}{\sqrt{2}}(\sigma_x + \sigma_z)$ and Pauli matrices σ_i. Their explicit expressions depend on the ordering of the four physical qubits, namely $\mathbf{k}_A$, $\mathbf{k}_B$, π_A, π_B. In this work we use four different ordering:

$$\text{(a) } (1,2,3,4) = (\mathbf{k}_B, \mathbf{k}_A, \pi_A, \pi_B),$$
$$\mathcal{U} = \sigma_x H \otimes \sigma_z \otimes \mathbb{1} \otimes H$$
$$\text{(b) } (1,2,3,4) = (\pi_B, \pi_A, \mathbf{k}_A, \mathbf{k}_B),$$
$$\mathcal{U} = H \otimes \sigma_z \otimes \sigma_x \otimes \sigma_z H$$
$$\text{(c) } (1,2,3,4) = (\mathbf{k}_A, \mathbf{k}_B, \pi_B, \pi_A),$$
$$\mathcal{U} = \sigma_z H \otimes \sigma_x \otimes \mathbb{1} \otimes H$$
$$\text{(d) } (1,2,3,4) = (\pi_A, \pi_B, \mathbf{k}_B, \mathbf{k}_A),$$
$$\mathcal{U} = H \otimes \mathbb{1} \otimes \sigma_x \otimes \sigma_z H.$$

In the following we refer to these expressions depending on the logical operation we consider.

The general measurement apparatus, differently used to perform each operation, is sketched in Fig. 2 (see caption for details). The $\mathbf{k}$ modes corresponding to photons A or B, are, respectively, matched on the up and down side of a common 50:50 beam splitter (BS) (see inset).

Single qubit rotations.—In the one-way model a three-qubit linear cluster state is sufficient to realize arbitrary single qubit rotations [14]. According to the measurement basis for a generic qubit j, $|\varphi_\pm\rangle_j = \frac{1}{\sqrt{2}}(|0\rangle_j \pm e^{-i\varphi}|1\rangle_j)$, we define $s_j = 0$ ($s_j = 1$) when the $|\varphi_+\rangle_j$ ($|\varphi_-\rangle_j$) outcome is obtained. With the 4-qubit cluster in the computational basis ($|\Phi_4^{\text{lin}}\rangle$) any arbitrary single qubit rotation expressed as $|\chi_{\text{out}}\rangle = R_x(\beta)R_z(\alpha)|\chi_{\text{in}}\rangle$ [15] can be obtained by a three step procedure [cf. Fig. 1(a)]. The sequence of the measurement bases for the three qubits are the following: (I) $\{|0\rangle_1, |1\rangle_1\}$, which allows us to obtain a three-qubit linear cluster; (II) $|\alpha_\pm\rangle_2$; (III) $|\beta_\pm\rangle_3$ or $|-\beta_\pm\rangle_3$, depending on the second qubit output $s_2 = 0$ or $s_2 = 1$, respectively. In the previous expression $R_z(\alpha) = \exp(-\frac{i}{2}\alpha\sigma_z)$, $R_x(\beta) = \exp(-\frac{i}{2}\beta\sigma_x)$ and $|\chi_{\text{in}}\rangle = |+\rangle(|-\rangle)$ if the output of the first measurement is $|0\rangle_1(|1\rangle_1)$. The output state $|\chi_{\text{out}}\rangle$ is created up to Pauli errors ($\sigma_x^{s_3}\sigma_z^{s_2}$), that should be corrected by proper FF operations for deterministic QC [4].

Let us consider ordering (a), where qubit $1 = \mathbf{k}_B$, qubit $2 = \mathbf{k}_A$, qubit $3 = \pi_A$, and qubit $4 = \pi_B$. The output state, encoded in the polarization of photon B, can be written in the laboratory basis as

$$|\chi_{\text{out}}\rangle_{\pi_B} = \sigma_z^{s_{\pi_A}}\sigma_x^{s_{\mathbf{k}_A}} H R_x(\beta)R_z(\alpha)|\chi_{\text{in}}\rangle, \qquad (3)$$

where the H gate derives from the change between the computational and laboratory basis. This also implies that the actual measurement bases are $|\pm\rangle_{\mathbf{k}_B}$ for the momentum of photon B (qubit 1) and $|\alpha_\mp\rangle_{\mathbf{k}_A}$ for the momentum of photon A (qubit 2). The measurement basis on the third qubit (π_A) depends, according to the one-way model, on the results of the measurement on the second qubit ($\mathbf{k}_A$). These are precisely what we call FF measurements [type (i)], corresponding in this scheme to measure π_A in the bases $|\beta_\pm\rangle_{\pi_A}$ or $|-\beta_\pm\rangle_{\pi_A}$, depending on the BS output mode (i.e., $s_{\mathbf{k}_A} = 0$ or $s_{\mathbf{k}_A} = 1$). Note that these deterministic FF measurements directly derive from the possibility of encoding two qubits ($\mathbf{k}_A$ and π_A) in the same photon. Differently from the case of 4-photon cluster states, this avoids the need of Pockels cells to perform active FF measurements, as was already stated.

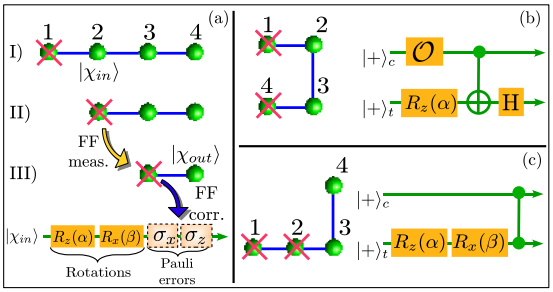

FIG. 1 (color online). (a) Top: Measurement pattern for arbitrary single qubit rotations on a 4-qubit linear cluster state, carried out in three steps (I, II, III). In each measurement, indicated by a red cross, the information travels from left to right. Feed-forward measurements and corrections are, respectively, indicated by the gray (yellow) and black (blue) arrows. Bottom: Equivalent logical circuit. (b) C-NOT realization via measurement of qubits 1, 4 on the horseshoe cluster (left) and equivalent circuit (right). (c) Universal C-PHASE gate realization via measurement of qubits 1 and 2 (left) and equivalent circuit (right).

Pauli errors FF corrections are in any case necessary for deterministic one-way QC. They were realized by using the measurement apparatus shown in Fig. 2. Here two fast driven transverse $LiNbO_3$ Pockels cells (σ_x and σ_z) with rise time $= 1n$ sec and $V_{\lambda/2} \sim 1$ kV are activated by the output signals of detectors a_i ($i = 1, 3, 4$) corresponding to the different values of s_{π_A} and $s_{\mathbf{k}_A}$. They perform the operation $\sigma_z^{s_{\pi_A}}\sigma_x^{s_{\mathbf{k}_A}}$ on photon B, coming from the output $s_{\mathbf{k}_B} = 0$ of BS and transmitted through a single mode optical fiber. Note that no correction is needed when photon A is detected on the output a_2 ($s_{\pi_A} = s_{\mathbf{k}_A} = 0$). Temporal synchronization between the activation of the high voltage signal and the transmission of photon B through the Pockels cells is guaranteed by suitable choice of the delays D. We used only one BS output of photon B, namely $s_{\mathbf{k}_B} = 0$, in order to perform the algorithm with initial state $|\chi_{\text{in}}\rangle = |+\rangle$. The other BS output corresponds to the algorithm starting with the initial state $|\chi_{\text{in}}\rangle = |-\rangle$.

In Fig. 3 the values of the output state fidelity obtained with or without active FF corrections (i.e., turning on or off the Pockels cells) are compared for different values of α

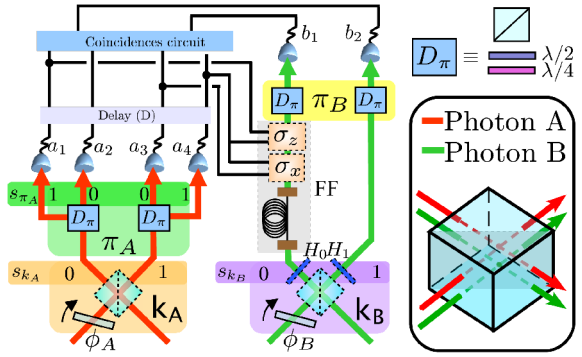

FIG. 2 (color online). Measurement setup for photons A and B. Momentum qubits $\mathbf{k}_A$ and $\mathbf{k}_B$ are measured by two thin glass plates (ϕ_A, ϕ_B), acting as phase shifters and inserted before the BS. Polarization qubits π_A and π_B are measured by standard tomographic setup, indicated by D_π. BS and D_π outputs are indicated by $s_j = 0, 1$, where the index j refers to the corresponding DOFs. Hadamard gates $H_{0,1}$ are realized by half wave plates. FF correction apparatus [used only with ordering (a)] is given by a 35 m length single mode fiber and two Pockels cells (σ_x, σ_z) driven by the output signals of detector a_1, a_3, a_4. Dashed lines for $H_{0,1}$, BS, and FF correction apparatus indicate that these devices can be inserted or not in the setup depending on the measurement. Inset: Spatial mode matching on the BS.

and β. The expected theoretical fidelities in the no-FF case are also shown. In all the cases the computational errors are corrected by the FF action, with average measured fidelity $F = 0.867 \pm 0.018$. The overall repetition rate is about 500 Hz, which is more than 2 orders of magnitude larger than one-way single qubit rotation realized with 4-photon cluster states.

We demonstrated the computational equivalence of the two DOFs of photon B by performing the same algorithm

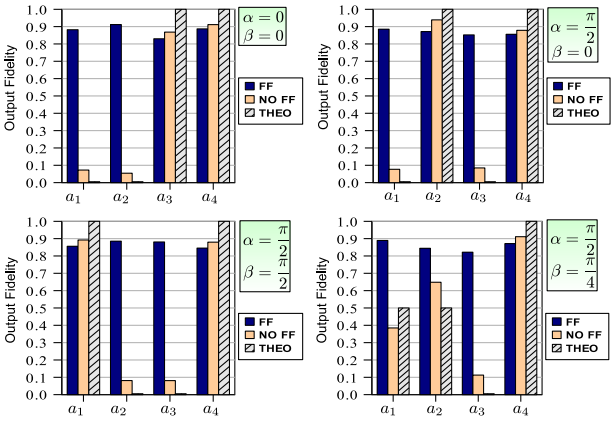

FIG. 3 (color online). Output fidelities of the single qubit rotation algorithm with [FF, black (blue) columns] or without [NO FF, gray (orange) columns] feed forward. In both cases, the four columns of the histogram refer to the measurement of the output state (encoded in the polarization of photon B) by detector b_1 in coincidence with $a_1, \ldots, a_4$, respectively. Gray dashed columns (THEO) correspond to theoretical fidelities in the no-FF case.

with ordering (b). In this case the explicit expression of the output state $|\chi_{\text{out}}\rangle_{\mathbf{k}_B}$ in the laboratory basis is $|\chi_{\text{out}}\rangle_{\mathbf{k}_B} = (\sigma_z)^{s_3}(\sigma_x)^{s_2}\sigma_z HR_x(\beta)R_z(\alpha)|\chi_{\text{in}}\rangle$. By using only detectors a_2, a_3, b_1, b_2 in Fig. 2 we measured $|\chi_{\text{out}}\rangle_{\mathbf{k}_B}$ choosing different values of α (which correspond in the laboratory to the polarization measurement bases $|\alpha_{\mp}\rangle_{\pi_A}$) and $\beta = 0$ (which correspond in the laboratory to the momentum bases $|-\beta_{\pm}\rangle_{\mathbf{k}_A}$). The first qubit ($\pi_B$) was always measured in the basis $|\pm\rangle_{\pi_B}$. By performing the $\mathbf{k}_B$ tomographic analysis for all the possible values of $s_2 \equiv s_{\pi_A}$ and $s_3 \equiv s_{\mathbf{k}_A}$ and of the input qubit (i.e., for different values of $s_1 \equiv s_{\pi_B}$) we obtained an average value of fidelity $F > 0.9$ (see Table I). In this case the realization of FF corrections could be realized by the adoption of active phase modulators. The (π)-($\mathbf{k}$) computational equivalence and the use of active feed forward show that the multi-degree of freedom approach is feasible for deterministic one-way QC.

C-NOT *gate for equatorial qubits.*—Nontrivial two-qubit operations, such as the C-NOT gate, can be realized by the four-qubit horseshoe (180° rotated) cluster state [see Fig. 1(b)], whose explicit expression is equal to $|\Phi_4^{\text{lin}}\rangle$. By simultaneously measuring qubits 1 and 4, it is possible to implement the logical circuit shown in Fig. 1(b). In the computational basis the input state is $|+\rangle_c \otimes |+\rangle_t$ (c, control; t, target), while the output state, encoded in qubits 2 (control) and 3 (target), is $|\Psi_{\text{out}}\rangle = H_t\text{C-NOT}(\mathcal{O}|+\rangle_c \otimes R_z(\alpha)|+\rangle_t)$ (for $s_1 = s_4 = 0$). In the above expression we have $\mathcal{O} = \mathbb{1}$ ($\mathcal{O} = H$) when qubit 1 is measured in the basis $\{|0\rangle_1, |1\rangle_1\}$ ($|\pm\rangle_1$). Qubit 4 is measured in the basis $|\alpha_{\pm}\rangle_4$. It is worth noting that this circuit realizes the C-NOT gate (up to the Hadamard H_t) for arbitrary equatorial target qubit and control qubit $|0\rangle$, $|1\rangle$, or $|\pm\rangle$ depending on the measurement basis of qubit 1.

The experimental realization of this gate was performed by adopting ordering (c). In this case the control output qubit is encoded in the momentum $\mathbf{k}_B$, while the target output is encoded in the polarization π_B. In the actual experiment we inserted H_0 and H_1 on photon B to compensate H_t. The output state in the laboratory basis is then

$$|\Psi_{\text{out}}\rangle = (\Sigma)^{s_4}\sigma_x^{(c)}\text{C-NOT}(\mathcal{O}\sigma_z^{s_1}|+\rangle_c \otimes R_z(\alpha)|+\rangle_t), \quad (4)$$

where all the possible measurement outcomes of qubits 1

TABLE I. Momentum ($\mathbf{k}_B$) experimental fidelities (F) of single qubit rotation output states for different values of α and $\beta = 0$. Each datum is obtained by the measurements of the different Stokes parameters, each one lasting 10 sec.

$\alpha(\beta = 0)$	F ($s_2 = s_3 = 0$)	F ($s_2 = 0$, $s_3 = 1$)
0	0.961 ± 0.003	0.971 ± 0.003
$\pi/2$	0.879 ± 0.006	0.895 ± 0.005
$\pi/4$	0.998 ± 0.005	0.961 ± 0.006
$-\pi/4$	0.833 ± 0.007	0.956 ± 0.006

TABLE II. Experimental fidelity (F) of C-NOT gate output target qubit for different value of α and $\mathcal{O}$.

$\mathcal{O}$	α	Control output	F ($s_4 = 0$)	F ($s_4 = 1$)
H	$\pi/2$	$s_1 = 0 \rightarrow \|1\rangle_c$	0.965 ± 0.004	0.975 ± 0.004
		$s_1 = 1 \rightarrow \|0\rangle_c$	0.972 ± 0.004	0.973 ± 0.004
	$\pi/4$	$s_1 = 0 \rightarrow \|1\rangle_c$	0.995 ± 0.008	0.902 ± 0.012
		$s_1 = 1 \rightarrow \|0\rangle_c$	0.946 ± 0.010	0.945 ± 0.009
$\mathcal{O}$	α	Control output	F ($s_1 = s_4 = 0$)	F ($s_1 = 0, s_4 = 1$)
$\mathbb{1}$	$\pi/2$	$\|0\rangle_c \equiv \|\ell\rangle_{\mathbf{k}_B}$	0.932 ± 0.004	0.959 ± 0.003
		$\|1\rangle_c = \|r\rangle_{\mathbf{k}_B}$	0.941 ± 0.005	0.940 ± 0.005
	$\pi/4$	$\|0\rangle_c = \|\ell\rangle_{\mathbf{k}_B}$	0.919 ± 0.007	0.932 ± 0.007
		$\|1\rangle_c = \|r\rangle_{\mathbf{k}_B}$	0.878 ± 0.009	0.959 ± 0.006

and 4 are considered. The Pauli errors are $\Sigma = \sigma_z^{(c)}\sigma_z^{(t)}$, while the matrix $\sigma_x^{(c)}$ is due to the change between the computational and laboratory bases. Table II shows the experimental fidelities of the target qubit corresponding to the measurement of the output control qubit in the basis $\{|0\rangle, |1\rangle\}$.

Universal C-PHASE *gate.*—We realized a C-PHASE gate for arbitrary target qubit and fixed control $|+\rangle_c$ [see Fig. 1(c)] by measuring qubits 1 and 2 of $|\Phi_4^{\text{lin}}\rangle$ in the bases $|\alpha_\pm\rangle$ and $|(-)^{s_1}\beta_\pm\rangle$, respectively. By considering ordering (d) we encoded the output state in the physical qubits $\mathbf{k}_A$ and $\mathbf{k}_B$. For $s_1 = s_2 = 0$, by using the appropriate base changing, the output state is written as

$$|\Psi_{\text{out}}\rangle = |-\rangle_{\mathbf{k}_A} \otimes \sigma_x|\Phi\rangle_{\mathbf{k}_B} + |+\rangle_{\mathbf{k}_A} \otimes \sigma_x\sigma_z|\Phi\rangle_{\mathbf{k}_B}. \quad (5)$$

Here $|\Phi\rangle_{\mathbf{k}_B} = R_x(\beta)R_z(\alpha)|+\rangle$ and the matrix σ_x is due to the basis changing. We measured the fidelity of target $\mathbf{k}_B$ corresponding to a control $|+\rangle_{\mathbf{k}_A}$ ($|-\rangle_{\mathbf{k}_A}$) for different values of α and β, obtaining an average value $F = 0.907 \pm 0.010$ ($F = 0.908 \pm 0.011$).

In conclusion, by using 2-photon 4-qubit cluster states, we realized arbitrary single qubit rotations, either probabilistic or deterministic, and fundamental two-qubit gates, such as a C-NOT gate for target qubits located in the equatorial plane of the Bloch sphere and a C-PHASE gate for generic target qubits. These operations were performed with high fidelity and at repetition rates which are 2 or even 3 orders of magnitude larger than those obtained with 4-photon cluster states. A more powerful task can be realized by increasing the information content of a quantum state. For instance, with 6 qubits a C-NOT gate operating over the entire Bloch sphere of the target and control qubits can be implemented. Other complex gates and algorithms require one to work with even more qubits [14]. This could be realized by using other DOFs, such as time-energy, or using a larger number of $\mathbf{k}$ modes within the emission cone of a type I crystal. This number scales exponentially with the number of qubits; however, up to eight qubits are feasible with two photons by using four modes per photon, besides polarization and time bin. At the same time, by operating with four photons eight-qubit cluster states could be generated by linking together two $|C_4\rangle$ states by a proper C-PHASE gate. It is worth noting that by encoding qubits into many spatial modes of the photons the complexity of the interferometric apparatus on which the system is based may increase. On the other hand, by this scheme the problems of detection efficiency of multiphoton cluster states are less severe. Indeed, for a given number Q of qubits, the efficiency scales as $\eta^{Q/M}$ with the number M of DOFs encoded in each photon. The efficiency gain offered by the multidegree of freedom with respect to the multiphoton approach compensates the difficulties arising from the apparatus complexity for values of efficiency for each photon ($\eta \sim 0.3$) typically available with the current technology. Hence a "hybrid" approach based on a multiphoton-multiqubit architecture may represent a solution to one-way QC in a midterm perspective.

Thanks are due to Fabio Sciarrino for useful discussions and Marco Barbieri for his contribution in planning the experiment. This work was supported by the contract PRIN 2005 of MIUR (Italy).

*http://quantumoptics.phys.uniroma1.it

†Present address: Université de Genève GAP-Optique, Rue de l'École-de-Mèdecine 20, CH-1211 Genève 4, Switzerland.

[1] R. Raussendorf and H. J. Briegel, Phys. Rev. Lett. **86**, 5188 (2001).
[2] E. Knill, R. Laflamme, and G. J. Milburn, Nature (London) **409**, 46 (2001).
[3] P. Walther *et al.*, Nature (London) **434**, 169 (2005).
[4] R. Prevedel *et al.*, Nature (London) **445**, 65 (2007).
[5] K. Chen *et al.*, Phys. Rev. Lett. **99**, 120503 (2007).
[6] G. Vallone *et al.*, Phys. Rev. Lett. **98**, 180502 (2007).
[7] Here "deterministic" refers to the success of the one-way algorithm and not to the overall process because of the random generation of spontaneous parametric down-conversion pairs.
[8] M. Barbieri, C. Cinelli, P. Mataloni, and F. De Martini, Phys. Rev. A **72**, 052110 (2005).
[9] M. Barbieri *et al.*, Phys. Rev. Lett. **97**, 140407 (2006).
[10] C. Cinelli *et al.*, Phys. Rev. Lett. **95**, 240405 (2005).
[11] The state (1) is equivalent to that generated in [6] up to single qubit transformations.
[12] N. Kiesel *et al.*, Phys. Rev. Lett. **95**, 210502 (2005).
[13] The state $|\Phi_4^{\text{lin}}\rangle$ is obtained by preparing a chain of qubits all prepared in the state $|+\rangle$ and then applying the gate $CP = |0\rangle\langle 0| \otimes \mathbb{1} + |1\rangle\langle 1| \otimes \sigma_z$ for each link.
[14] R. Raussendorf, D. E. Browne, and H. J. Briegel, Phys. Rev. A **68**, 022312 (2003); M. S. Tame, M. Paternostro, M. S. Kim, and V. Vedral, Phys. Rev. A **72**, 012319 (2005).
[15] Three sequential rotations are necessary to implement a generic $SU(2)$ matrix but only two, namely $R_x(\beta)R_z(\alpha)$, are sufficient to rotate the input state $|\chi_{\text{in}}\rangle = |\pm\rangle$ into a generic state.